

NicheFlow: Towards a foundation model for Species Distribution Modelling

Russell Dinnage¹

¹Florida International University

October 15, 2024

¹ Abstract

1. Species distribution models (SDMs) are crucial tools for understanding and predicting biodiversity patterns, yet they often struggle with limited data, biased sampling, and complex species-environment relationships. Here I present NicheFlow, a novel foundation model for SDMs that leverages generative AI to address these challenges and advance our ability to model and predict species distributions across taxa and environments.
2. NicheFlow employs a two-stage generative approach, combining species embeddings with two chained generative models, one to generate a distribution in environmental space, and a second to generate a distribution in geographic space. This architecture allows for the sharing of information across species and captures complex, non-linear relationships in environmental space. I trained NicheFlow on a comprehensive dataset of reptile distributions and evaluated its performance using both standard SDM metrics and zero-shot prediction tasks.
3. NicheFlow demonstrates good predictive performance, particularly for rare and data-deficient species. The model successfully generated plausible distributions for species not seen during training, showcasing its potential for zero-shot prediction. The learned species embeddings captured meaningful ecological information, revealing patterns in niche structure across taxa, latitude and range sizes.
4. As a proof-of-principle foundation model, NicheFlow represents a significant advance in species distribution modeling, offering a powerful tool for addressing pressing questions in ecology, evolution, and conservation biology. Its ability to model joint species distributions and generate hypothetical niches opens new avenues for exploring ecological and evolutionary questions, including ancestral niche reconstruction and community assembly processes. This approach has the potential to transform our understanding of biodiversity patterns and improve our capacity to predict and manage species distributions in the face of global change.

²¹ **Keywords:** biodiversity, deep learning, ecological niche, foundation models, generative AI, species distribution modeling,
²² zero-shot prediction

²³ Introduction

²⁴ The accelerating pace of environmental change has amplified the need for accurate species distribution
²⁵ predictions, a cornerstone of biodiversity conservation, ecological research, and informed management

26 decisions. Species distribution models (SDMs) have become indispensable tools for mapping and fore-
27 casting species occurrences under current and future conditions, playing a crucial role in efforts to
28 mitigate the impacts of habitat loss, climate change, and other anthropogenic pressures. However, tra-
29 ditional SDMs often stumble when confronted with rare or data-deficient species, typically demanding
30 substantial occurrence data and leading to repetitive, species-specific modeling efforts across research
31 groups and conservation practitioners (Guisan et al., 2017).

32 Conventional SDMs, such as Maxent, Generalized Linear Models (GLMs), and Random Forests (RF),
33 rely heavily on species-specific occurrence records and environmental variables to estimate species-
34 environment relationships (Elith & Leathwick, 2009). These models often operate under the assumption
35 that species niches are determined solely by current environmental conditions, aligning with the envi-
36 ronmental niche concept that defines a species' fundamental ecological space based on its abiotic and
37 biotic requirements (Soberón, 2007). However, the variability in availability and quality of occurrence
38 data can lead to biased or incomplete predictions, particularly for rare, cryptic, or newly discovered
39 species (Yackulic et al., 2013).

40 The emergence of foundation models in ecology, particularly those leveraging generative AI approaches,
41 offers a paradigm shift: a unified model capable of generating distribution predictions for hundreds of
42 thousands of species, including those absent from its training data. This approach not only streamlines
43 the modeling process but also unlocks the potential for robust predictions in the face of limited data, a
44 common challenge in biodiversity research (Beery et al 2021).

45 **Unlocking the potential of foundation models in Ecology and Conservation**

46 The potential of foundation models in ecology extends far beyond mere prediction. These models, which
47 have revolutionized fields like natural language processing and computer vision (Bommasani et al., 2021),
48 offer a suite of advantages that could transform ecological research:

49 1. Reduction of Duplicated Effort: A unified foundation model allows movement beyond the fragmen-
50 ted landscape of species-specific models, enabling collective progress and ensuring consistency across
51 predictions (Pimm et al., 2015; Franklin, 2013).

52 2. Computational Efficiency: Pre-trained models significantly reduce the computational demands of
53 SDMs, an increasingly important consideration given the rising concerns over the carbon footprint of
54 machine learning (Strubell et al., 2019; Patterson & Hennessy, 2021).

55 3. Democratization of Advanced Techniques: By simplifying the modeling process, foundation models
56 can make sophisticated analytical tools accessible to ecologists with limited machine learning expertise,
57 broadening the community of researchers who can contribute to and benefit from cutting-edge SDM
58 techniques (Beery et al. 2021).

59 4. Collaborative Model Improvement: A unified model fosters a cycle of iterative improvement, where
60 each user builds upon the work of others, enhancing model performance over time (Pereira et al., 2010).
61 In this paper, I present a novel approach that combines generative AI with species embeddings derived
62 from distribution data, enabling zero-shot predictions in SDMs without requiring explicit trait or phylo-
63 genetic information. This method builds upon recent advances in machine learning, particularly in the
64 fields of generative modeling and representation learning (Reichstein et al., 2019; Ho et al., 2020). By
65 learning latent representations of ecological niches, the model aligns with the concept that niches are
66 defined by where a species occurs relative to environmental gradients (Soberón, 2007).

67 **Enabling Zero-shot Species Distribution Prediction**

68 An exciting aspect of foundation models is their capacity for few-shot and zero-shot learning. Few-shot
69 learning refers to the ability of a model to make accurate predictions with very limited training data for a
70 particular task or category (Wang et al., 2020). Zero-shot learning goes a step further, allowing models
71 to make predictions for entirely new categories that were not present at all in the training data (Xian
72 et al., 2018). These concepts, while originating from machine learning, have profound implications for
73 ecology. In the context of SDMs, zero-shot learning would enable predictions of species distributions for
74 which we have no occurrence data in our training set. This capability is analogous to an experienced
75 ecologist making an educated guess about where a newly discovered species might occur based on
76 its taxonomic relationships and the known distributions of similar species (Lampert et al., 2014). For
77 SDMs, this means we could potentially predict distributions for rare, newly discovered, or data-deficient
78 species by leveraging the model's learned representations of ecological niches and species-environment
79 relationships across a wide range of taxa (Norberg et al., 2019).

80 **Capturing ecological meaning**

81 The model I present here goes beyond traditional Joint Species Distribution Models (JSDMs) by captu-
82 ring the "distribution of distributions" that is, the underlying environmental niches of species. Instead of
83 focusing on the residual covariance among species, as in linear JSDMs (Pollock et al., 2014; Ovaskainen
84 et al., 2016), this generative AI approach seeks to learn the distribution of ecological niches directly
85 from occurrence data. This allows for the estimation of complex, multidimensional patterns that define
86 species' environmental tolerances with a flexibility and power that surpasses traditional JSDMs (Norberg
87 et al., 2019).

88 Beyond its predictive applications, the species embeddings generated by this model serve as a powerful
89 research tool, encoding ecological niches in a way that allows for downstream analyses such as estimating
90 ecological distances between species, reconstructing ancestral niches, or querying for species with similar
91 environmental tolerances. This functionality provides a unique opportunity to explore the ecological

92 dimensions of biodiversity, deepening our understanding of species' fundamental and realized niches and
93 their evolutionary implications (Soberón & Peterson, 2005).

94 In the following sections, I detail the technical implementation of this approach, present results de-
95 monstrating its performance on both seen and unseen species, and discuss the broader implications for
96 ecological research and biodiversity conservation. This work represents a significant step towards unify-
97 ing species distribution knowledge into a single, powerful predictive framework, opening new avenues
98 for addressing pressing ecological challenges and advancing our understanding of biodiversity patterns
99 and processes.

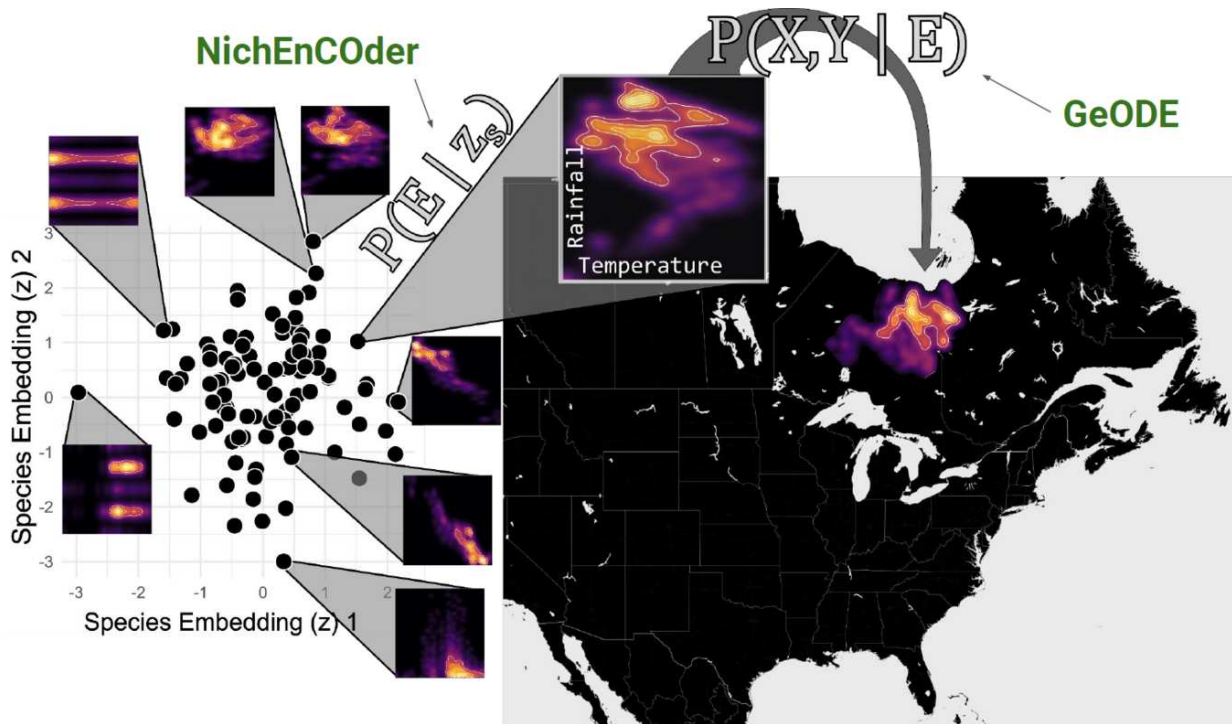


Figure 1: Conceptual illustration of the two step generative AI model for Joint Species Distribution Modeling called NicheFlow, proposed in this study. A generative model of the species environmental niche (NichEncoder) is composed with a generative model mapping environmental variables to geographic coordinates (GeODE). (GeODE). A species environmental niche is represented by a d-dimensional vector z that is transformed into a k-dimensional environmental probability distribution or hypervolume. A z vector for every species is estimated during model training and provides a generalizable, reusable compact representation of species's niches. Across all species the distribution of z represents the 'distribution of (environmental) distributions'.

100 Methods

101 Generative Model Framework for Joint Species Distribution Modeling

102 I develop a generative approach to species distribution modeling that integrates species-specific infor-
103 mation and environmental conditions through probabilistic models. This approach allows us to capture
104 complex ecological relationships by linking species occurrences with environmental variables and geo-
105 graphic coordinates.

106 Model Equation

107 In order to create a usable generative model for species distribution modeling it needs to have a target
108 probability distribution to generate from. To create a map of species the goal is to sample from the
109 probability distribution of species across geographic coordinates (X, Y) , given that the species is $S = s$,
110 and that it occurs ($O_s = 1$) e.g. $P(X, Y | S = s, O_s = 1)$. We further need to condition on species in
111 a quantitative generalizable way. To do this, instead of conditioning on the identity of a species, we
112 can condition on a vector representation of the species's niche, a latent vector-valued variable we will
113 call Z , which will be estimated by the model along with the other parameters. For simplicity I will use
114 the expression $Z = z_s$ to represent $S = s, O_s = 1$, leaving us with $P(X, Y | Z = Z_s)$. To include this
115 latent niche vector and also the environment in our probability of interest, we can use the law of total
116 probability to arrive at the following mathematical representation:

$$P(X, Y | S = s) = \int_{-\infty}^{\infty} \cdots \int_{-\infty}^{\infty} P(X, Y | \mathbf{E}) \left(\int_Z P(\mathbf{E} | \mathbf{Z} = \mathbf{z}_s) P(\mathbf{Z}) dz \right) de_1 \cdots de_n. \quad (1)$$

117 This equation shows how the occurrence of a species can be modeled by chaining two probability
118 distributions: one that describes the species' environmental niche ($P(\mathbf{E} | Z = z_s)$) and another that
119 links environmental conditions to geographic space ($P(X, Y | \mathbf{E})$). Figure 1 shows this two-step
120 sampling process conceptually. By learning a representation of the species niche as a latent variable
121 Z_s , we can create a flexible model that captures both the environmental dependencies and geographic
122 patterns of species distributions. The distribution of z represents the 'distribution of distributions'. More
123 specifically, the distribution across species of distributions in environmental and geographic space. See
124 the supporting information for the full derivation of equation 1.

125 Sampling from the Species Distribution Using Generative Models

126 The equations derived above describe the probability of species occurrences as complex high-dimensional
127 integrals that are computationally expensive to evaluate directly. To overcome this challenge, I leverage
128 generative models, which can efficiently approximate these distributions by sampling, thus bypassing the
129 need to compute these integrals explicitly.

130 **Generative Model Framework for Sampling**

131 Generative models, such as Variational Autoencoders (VAEs) and rectified flow models, provide a pow-
132 erful framework for approximating high-dimensional probability distributions through sampling. These
133 models learn to generate data that resemble the distribution of the observed data by learning the
134 underlying data-generating process.

135 **1. Sampling from the Environmental Niche:**

136 From Equation (3), the term $P(\mathbf{E} | \mathbf{Z} = \mathbf{z}_s)$ represents the species' environmental niche. We can
137 use a generative model to learn this niche distribution by training it on environmental data asso-
138 ciated with species occurrences. Once trained, the model can generate samples of environmental
139 vectors \mathbf{E} conditioned on the species embedding $\mathbf{Z} = \mathbf{z}_s$.

140 **Model Training:** I train a generative model called **NichEncoder**, using a two-stage generative
141 model – combination of a Condition Variation Autoencoder (CVAE; Zheng et al. 2023) and a
142 Rectified Flow model (Liu et al. 2023). The model is trained using environmental occurrence
143 data for many species. The model learns a mapping from a latent space (representing \mathbf{Z}) to
144 the environmental conditions that define species niches. See 'Model Details' for more details of
145 NichEncoder.

146 **Sampling:** After training, new environmental vectors \mathbf{E} can be generated by sampling from the
147 learned latent space. These samples represent possible environmental conditions under which the
148 species $S = s$ can occur.

149 **2. Sampling Geographic Coordinates Given Environmental Conditions:**

150 The next step involves generating geographic coordinates (X, Y) given the sampled environmental
151 conditions \mathbf{E} . The term $P(X, Y | \mathbf{E})$ describes this relationship and can also be modeled using a
152 generative approach.

153 **Training the Spatial Generative Model:** A second generative model is trained to map environ-
154 mental conditions \mathbf{E} to geographic coordinates. This model learns the spatial patterns of species
155 occurrences based on the environmental vectors generated in the previous step. The model is
156 called **GeODE**, and is based on a Conditional Rectified Flow model (Liu et al 2022). The name
157 is based on the fact that Rectified Flow models estimate an Ordinary Differential Equation to
158 transform noise into a complex high dimensional distribution. More details on **GeODE** can be
159 found in the 'Model Details' section.

160 **Sequential Sampling:** Once the spatial model is trained, it can sequentially generate coordi-
161 nates (X, Y) by conditioning on the sampled environmental vectors. This process allows us to
162 reconstruct the spatial distribution of the species without needing to evaluate the full integral.

163 **3. Combining the Sampling Steps:**

164 By chaining the two generative models, the overall sampling process approximates the species
165 distribution defined by Equation (3). Specifically:

- 166 • First, sample \mathbf{E} from the environmental niche model conditioned on $\mathbf{Z} = \mathbf{z}_s$.
- 167 • Then, use the sampled \mathbf{E} to generate corresponding coordinates (X, Y) using the spatial
168 generative model.

169 This approach provides a flexible and efficient method to approximate the distribution of species
170 occurrences, leveraging the generative model's capacity to learn complex, high-dimensional rela-
171 tionships between species, environment, and geography.

172 **Zero-shot Species Distribution Modeling**

173 Zero-shot Species Distribution Modeling (0-SDM) enables the estimation of geographic distributions for
174 species not included in the training set by optimizing a latent embedding specific to the new species.
175 This approach adjusts the embedding based on observed occurrence data by comparing predicted and
176 observed environmental vectors using Energy Distance and Sinkhorn Distance. These distance measures
177 provide a robust method for aligning predicted species distributions with observed data.

178 **Embedding Optimization**

179 For a new species $S = s^*$ not present in the training data, the goal is to find an optimal embedding \mathbf{z}_{s^*}
180 within the latent space learned by the generative models. This embedding is iteratively adjusted to fit
181 the observed environmental conditions of the new species.

182 **Steps of the Optimization Process:**

183 **1. Initialization:**

184 The species embedding \mathbf{z}_{s^*} is initialized either randomly from the prior distribution $P(\mathbf{Z})$ or based
185 on similarities to embeddings of known species with similar ecological traits.

186 **2. Sampling Environmental Conditions:**

187 The environmental generative model, defined as the function f_{env} , is used to sample predicted
188 environmental vectors $\mathbf{e}_{\text{pred}}^{\mathbf{z}_{s^*}}$ conditioned on the embedding \mathbf{z}_{s^*} :

$$\mathbf{e}_{\text{pred}}^{\mathbf{z}_{s^*}} = f_{\text{env}}(\mathbf{z}_{s^*}), \quad \text{where } \mathbf{e}_{\text{pred}}^{\mathbf{z}_{s^*}} \sim P(\mathbf{E} \mid \mathbf{Z} = \mathbf{z}_{s^*}).$$

189 Here, f_{env} maps the species embedding to predicted environmental conditions, capturing the
190 species' ecological niche in the environmental space.

3. **Loss Calculation Using Energy Distance and Sinkhorn Distance:** To optimize the embedding \mathbf{z}_{s^*} , we define a loss function that evaluates how well the predicted environmental vectors \mathbf{E}_{pred} align with the observed environmental vectors \mathbf{E}_{true} from occurrence data. Here, \mathbf{E}_{pred} and \mathbf{E}_{true} are matrices where rows represent individual environmental vectors associated with predicted and observed occurrences, respectively. These matrices can have different numbers of rows, reflecting the flexibility of the distance measures used. The overall loss function used for optimization is defined as:

$$\mathcal{L}(\mathbf{z}_{s^*}) = \alpha \cdot E(\mathbf{E}_{\text{pred}}, \mathbf{E}_{\text{true}}) + (1 - \alpha) \cdot S(\mathbf{E}_{\text{pred}}, \mathbf{E}_{\text{true}}).$$

191 where E is Energy Distance (Székely & Rizzo, 2013) and S is the Sinkhorn Distance (Cuturi, 192 2013). Both are metric designed to estimate the similarity of two distribution expressed as point 193 clouds. Using a combination of both balances their different strengths. See Supporting Information 194 for details on Energy and Sinkhorn Distance including their equations, and optimization details.

4. **Optimization of the Species Embedding:** The species embedding \mathbf{z}_{s^*} is optimized using stochastic gradient descent (SGD) to minimize the combined loss $\mathcal{L}(\mathbf{z}_{s^*})$. The iterative updates refine the embedding until the generated environmental predictions closely match the observed environmental data. ##### Optimization Update:

$$\mathbf{z}_{s^*}^{(t+1)} = \mathbf{z}_{s^*}^{(t)} - \eta \nabla_{\mathbf{z}_{s^*}} \mathcal{L}(\mathbf{z}_{s^*}),$$

195 where η is the learning rate, and $\nabla_{\mathbf{z}_{s^*}} \mathcal{L}$ is the gradient of the loss function with respect to the 196 embedding.

197 **NichEncoder: Generative Model for Species Environmental Niches**

198 NichEncoder is a two-stage generative model designed to estimate species-specific environmental niches. 199 It takes as input a vector of latent species embeddings, $\mathbf{z}_{\text{species}}$, and generates environmental variables, 200 \mathbf{e} , representing the conditions associated with species occurrences. This approach allows the model 201 to learn complex, non-linear relationships between species and their environmental contexts, facilitating 202 predictions of species distributions in novel scenarios. The model was implemented in R using the torch 203 package, which provides a high-level interface to the PyTorch deep learning library.

204 **Model Architecture and Training**

205 NichEncoder follows a two-stage generative approach inspired by the Two-Stage VAE architecture (Dai 206 and Wipf, 2019), which is particularly useful for modeling complex, high-dimensional data distributions 207 with structured priors. This architecture allows for dimensionality reduction and disentanglement of the 208 latent space, improving the model's ability to capture the underlying data manifold. In the context of 209 NichEncoder, the first stage estimates the data manifold, and the second stage estimates the distribution

210 of the data on this manifold. For the first stage I used a conditional Variational Autoencoder (CVAE: 211 Zheng et. al 2023), and for the second stage I used a conditional Rectified Flow model (RF: Liu et 212 al. 2023), where the generative models are both conditioned on z_s , an estimated species-level latent 213 niche variable. Details of the architectures can be found in the Supporting Information.

214 **Model Training and Implementation**

215 Both stages of NichEncoder are trained sequentially using GPU acceleration with CUDA, with extensive 216 logging and periodic checkpointing to monitor training progress and performance. The implementation 217 of both stages was carried out in R using the `torch` package, which interfaces with the PyTorch library, 218 allowing efficient and flexible model training in a high-level language environment.

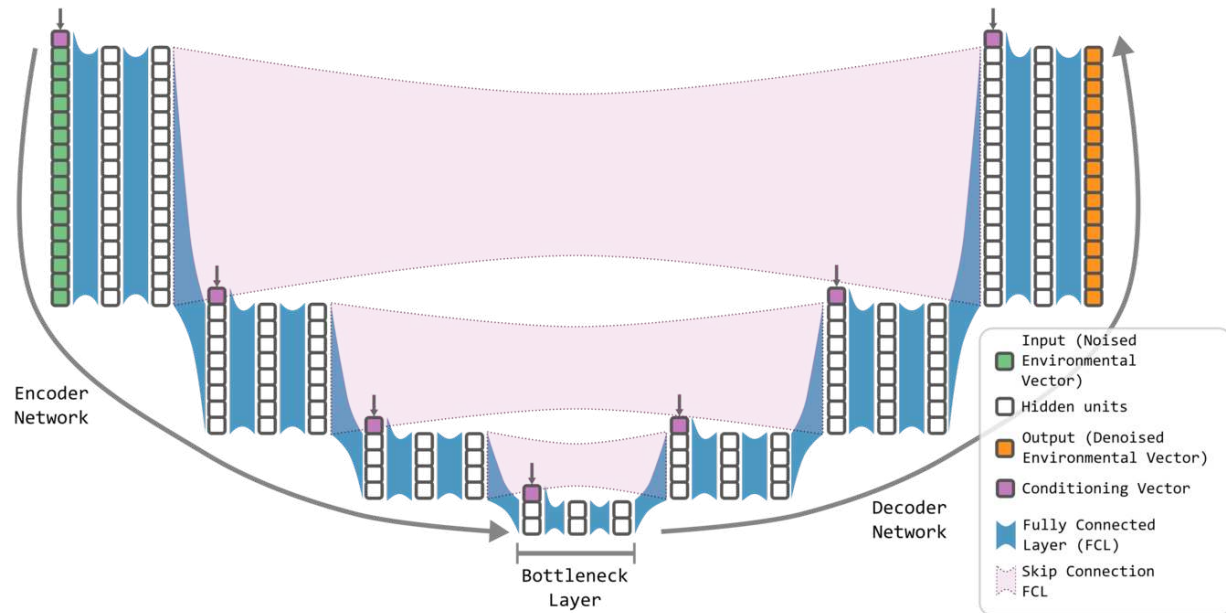


Figure 2: *Schematic representation of the modified U-Net architecture used in the Rectified Flow model.* The input to the network is a noised environmental vector (green), which undergoes a series of transformations through fully connected layers (blue blocks). The U-Net structure includes downsampling and upsampling paths, with hidden units (gray) processed at each layer. Skip connections (purple dashed lines) preserve feature information between corresponding layers, enhancing the model's ability to capture multi-scale patterns in the data. Conditioning vectors (pink) provide species-specific context at multiple stages, integrating key environmental and biological factors into the transformation. The output (orange) is the denoised environmental vector, representing a structured transformation from noise to the target distribution, guided by the learned vector field. This architecture supports efficient and accurate sampling within the Rectified Flow model, leveraging hierarchical feature extraction and integration across the network.

218

219

220 **GeODE: Generative Model for Geographic Distributions**

221 GeODE (Geographic Occurrence Distribution Estimator) is a generative model that employs a conditional
222 rectified flow to predict geographic distributions (Figure 1). The model outputs longitude (X) and
223 latitude (Y) coordinates by evolving a 2-dimensional noise vector toward the target distribution, which
224 represents species' occurrence points on the Earth's surface. The transformation is guided by an Ordinary
225 Differential Equation (ODE), which is conditioned on environmental vectors (e) corresponding to each
226 X, Y pair. Unlike the NichEncoder model, GeODE does not require an initial VAE step because the
227 output coordinates are already in a low-dimensional (2D) space, making the process more direct.

228 **Model Architecture**

229 GeODE uses a modified rectified flow architecture similar to that used in NichEncoder but tailored
230 specifically for geographic data. The model generates 2-dimensional noise vectors as inputs, which are
231 transformed through the rectified flow mechanism to output the desired geographic coordinates. The
232 input consists of random noise vectors representing initial guesses in 2D space, while the conditioning
233 input (e) comprises environmental variables associated with each geographic location. Each environ-
234 mental vector is normalized using means and standard deviations calculated from the data, ensuring
235 numerical stability during training.

236 **U-net Architecture**

237 The core of GeODE is a U-net style structure implemented with Multi-Layer Perceptrons (MLPs) in-
238 stead of convolutional layers (Figure 2). The U-net consists of two primary paths: downsampling and
239 upsampling. In the downsampling path, the input noise vectors and environmental conditioning are
240 passed through three fully connected layers with progressively smaller neuron counts (512, 256, and
241 128). These layers reduce the dimensionality while learning broad, high-level representations of the rela-
242 tionship between geographic locations and environmental factors. The upsampling path reconstructs the
243 geographic coordinates by reversing the dimensionality reduction, using three corresponding fully con-
244 nected layers to produce the final outputs. Skip connections between the downsampling and upsampling
245 paths retain and propagate finer details, leading to more accurate predictions.

246 **Input Conditioning and Encoding**

247 In addition to the U-net structure, GeODE includes specialized encoding layers for the time variable t and
248 environmental conditioning vectors. A linear layer encodes the time step, representing the interpolation
249 factor between noise and target coordinates. Another linear layer processes the environmental vectors,
250 embedding them into a latent space that informs the transformation from noise to geographic coordi-
251 nates. These encoded time and environmental vectors are concatenated with the latent representations
252 from the U-net, allowing the model to incorporate both spatial and environmental dependencies into its
253 predictions.

254 **Training Data Creation**

255 Training data for GeODE is generated through a Monte Carlo sampling process. Gaussian noise samples
256 are drawn for both the latitude and longitude dimensions, creating initial random coordinate sets. These
257 coordinates are linearly interpolated with target coordinates (actual occurrence points), guided by the
258 ODE. This interpolation path forms the input for training, allowing the model to learn how to evolve
259 from noise to realistic geographic distributions.

260 **Model Training and Implementation**

261 GeODE was implemented in R using the `torch` package, leveraging GPU acceleration with CUDA for
262 efficient training.

The full model that combines NichEncoder and GeODE to generate species distribution models was
named the **NicheFlow** model. It requires the training of 5 generative models that are chained together.
NichEncoder is composed of three models:

$$\text{NichEncoder}_{VAE} \rightarrow \text{NichEncoder}_{RF\curvearrowleft} \rightarrow \text{NichEncoder}_{RF\leftarrow}$$

263 Where VAE refers to the initial Variational Autoencoder model, $RF \curvearrowleft$ refers to the stage 1 Rectified
264 Flow model and $RF \leftarrow$ refers to the stage 2 Rectified Flow model, which has had its ODE rectified
265 (made linear). GeODE is composed of two models:

$$\text{GeODE}_{RF\curvearrowleft} \rightarrow \text{GeODE}_{RF\leftarrow}$$

266 These three models are chained and each needs to be trained on the output of the model to its immediate
267 left. This means that NichEncoder and GeODE can be trained in parallel, but the sub-models have
268 to be trained sequentially. I sequentially trained each of the sub-models in NichEncoder and GeODE
269 (in parallel), each on a Nvidia A100 GPU. Once trained the $RF \curvearrowleft$ models could be discarded and
270 the $RF \leftarrow$ used for the rectified flow part of the model. These models are much more computationally
271 efficient because they have been 'rectified', meaning they can be well approximated by only a single step
272 of ODE integration.

273 For the z_{species} latent space we set the dimension to 32. If fewer dimensions were needed the L2 penalty
274 apply to the loss would shrink some dimensions to effectively zero variance.

275 Utilizing multiple A100 GPUs to parallelize model training where it was possible, all 5
276 models that need to be trained to make up *NicheFlow* took less than 1 week to train
277 in total for 2,500 epochs, 6,000 epochs, 3,000 epochs, 5,000 epochs, and 2,000 epochs
278 for NichEncoder_{VAE} , $\text{NichEncoder}_{RF\curvearrowleft}$, $\text{NichEncoder}_{RF\leftarrow}$, $\text{GeODE}_{RF\curvearrowleft}$, and $\text{GeODE}_{RF\leftarrow}$, respec-
279 tively.

280 Model Evaluation

281 To evaluate the performance of the generative species distribution model (SDM), I compared model
282 predictions to observed test occurrence points using hexagonal binning and spatial aggregation. This
283 approach allowed us to transform the model's generative output into a comparable format for calculat-
284 ing standard SDM performance metrics, such as accuracy, ROC-AUC, and True Skill Statistic (TSS),
285 facilitating comparisons with other SDM approaches.

286 I tested the performance on 424 randomly selected species from the ~10,000 in the training dataset.
287 The random sampling was stratified by data deficiency (fewshot) status, three levels of geographic range
288 size (2.5 - 25 km², 25 - 220 km², and 220 - 2000 km²), and three levels of absolute mid-latitude (0 -
289 17 degrees, 17 - 34 degrees, 34 - 51 degrees), to get a geographically representative set of species. No
290 reptile species had an absolute mid-latitude greater than 51 degrees.

291 Hexagonal binning was used to approximate the probability of species occurrence across the study area.
292 The geographic predictions of the model, consisting of sampled points, were grouped into hexagonal
293 grid cells, creating an occurrence density map. The relative occurrence probability within each hex cell
294 was calculated as the proportion of predicted points within that hex compared to the total predicted
295 points across all hexes. This procedure allows the generative output, which produces samples rather than
296 explicit probabilities, to be converted into a spatially aggregated form that is comparable to traditional
297 SDMs that produce per-cell probabilities.

298 The evaluation was conducted within a more localized geographic context, which is a common approach
299 in traditional SDMs that typically model distributions within a “background area” — a region of interest
300 surrounding the species' known occurrence points. While NicheFlow, being a global model, is trained to
301 localize species distributions across the entire world, I confined its predictions to a smaller geographic
302 region to simulate the background area used in traditional SDMs. Specifically, I identified the set of
303 ecoregions overlapping the species' known occurrence points and used these ecoregions as the back-
304 ground area for evaluation. This approach allowed us to evaluate whether the model could accurately
305 localize the species within its natural ecoregions, which is a more fine-grained task compared to merely
306 determining the part of the world where the species is likely to occur.

307 I compared the predicted occurrence probabilities within these localized ecoregions to observed occur-
308 rence points. For each hexagonal cell, I calculated the proportion of observed occurrence points (from
309 test data) and used this as the “true” occurrence probability. The True Skill Statistic (TSS), also known
310 as Youden's J-index (Youden, 1950), was used as the primary evaluation metric to assess the model's
311 ability to differentiate between presence and absence cells.

312 In addition to TSS, I calculated several other standard SDM evaluation metrics, including Accuracy,
313 ROC-AUC, and F-measure. Accuracy is the proportion of correctly predicted presences and absences
314 across all hexes. ROC-AUC (Receiver Operating Characteristic - Area Under Curve) quantifies the

315 model's ability to discriminate between presence and absence, with values closer to 1 indicating better
316 discrimination. F-measure balances precision and recall in binary classification problems, providing a
317 robust metric for evaluating the presence/absence predictions across hexes.

318 To calibrate the model predictions, I applied a thresholding procedure (Phillips et al., 2006). The
319 generative model outputs continuous probabilities for each hexagonal cell, so a threshold is needed to
320 convert these probabilities into binary presence/absence predictions. I applied a threshold optimization
321 approach based on TSS, selecting the threshold that maximizes the TSS score for the test data. This
322 allowed us to determine the optimal cutoff for classifying a cell as occupied or not, improving model
323 interpretability and comparison with other SDM methods.

324 The evaluation process was implemented using the tidymodels framework (Kuhn and Wickham, 2020) for
325 calculating metrics and the probably package (Vaughan, 2020) for threshold optimization. Geographic
326 data manipulation and visualization were performed using the sf (Pebesma, 2018) and h3 (Brodrick,
327 2019) packages, ensuring accurate spatial alignment and efficient processing of hexagonal grids.

328 **Dataset**

329 **Species Distribution Data**

330 The dataset used to test the model consists of species distribution maps for 10,064 extant reptile species,
331 encompassing a wide variety of taxa, including lizards, snakes, turtles, amphisbaenians, and crocodiles
332 (Roll et al., 2017). These species distribution maps represent polygons of the species' extents of
333 occurrence, which were derived from a combination of sources, including field guides, museum databases,
334 the Global Biodiversity Information Facility (GBIF), the International Union for Conservation of Nature
335 (IUCN), and expert observations. This rich dataset provides comprehensive global coverage of reptile
336 distributions and is well-suited to train generative models for species distribution prediction.

337 For the purposes of this study, I transformed the polygonal data into point occurrences to better suit
338 the requirements of the generative modeling approach. Using the R package sf (Pebesma, 2018), I
339 uniformly sampled 800 points within each polygon to serve as the main training dataset. Additionally,
340 I created a held-out test set for each species by sampling a further 400 points, which were excluded
341 during training and used to evaluate the model's performance.

342 In addition to testing the model on species with abundant occurrence data, I specifically designed a set
343 of species to simulate real-world scenarios where distribution data is sparse. This subset, referred to as
344 the 'few-shot species,' includes species for which I only sampled 4 random points from their distribution.
345 This design choice allowed me to evaluate the model's capacity to learn distributions of species with
346 highly limited data—a situation that is frequently encountered in real biodiversity datasets. The few-shot
347 testing is an important component of evaluating the model's robustness to data deficiency.

348 Moreover, a subset of species was deliberately left out of the training set entirely to test the model's
349 zero-shot capabilities, as described in previous sections. This experimental design allows for a com-
350 prehensive evaluation of the model's ability to predict species distributions across a wide spectrum of
351 data availability, from well-sampled species to those for which no prior occurrence data was used during
352 training.

353 **Environmental Data**

354 In this study, I utilized the CHELSA-BIOCLIM dataset (Karger et al. 2017) to extract 32 environmental
355 variables crucial for species distribution modeling. These bioclimatic variables, which include mean
356 annual temperature, precipitation patterns, and seasonality, provide insights into the climatic factors
357 that shape species distributions (Karger et al., 2017). The high spatial resolution of 30 arc-seconds (~ 1
358 km 2) in the CHELSA-BIOCLIM dataset enables precise mapping of environmental conditions at species'
359 occurrence points, which is particularly useful in ecological niche modeling. Due to large amounts of
360 missing data in 2 of the 32 CHELSA-BIOCLIM variables (), these were subsequently dropped from the
361 training data used by NicheFlow.

362 To integrate the environmental data into the model, I used the `terra` package in R (Hijmans, 2022) to
363 extract these variables at specific spatial points corresponding to species occurrence locations.

364 **Results**

365 **NicheFlow captures a representation of niches**

366 After model training , I found 2 of the 32 dimensions that the model were initialized with shrank to near
367 zero variance during training so the effective dimension of the resulting latent species niche space was 30.
368 To visualize the structure of this latent niche space I used the UMAP algorithm (McInnes et al., 2018)
369 . UMAP (Uniform Manifold Approximation and Projection) is a dimensionality reduction technique that
370 helps visualize complex, high-dimensional data in two or three dimensions, while preserving important
371 structure and relationships between data points. It is widely used in biology for tasks such as visualizing
372 gene expression patterns, clustering species based on traits, or analyzing ecological datasets. UMAP is
373 particularly valued for its ability to capture both local and global data patterns more effectively than
374 older methods like PCA or t-SNE. I used it to reduce the 30 effective dimensions of the niche space to
375 2 for easy visualization (Figure \ref{985500})

376 I found that species were in some case widely separated in the two UMAP axes, appearing in multiple
377 clusters throughout the space. I also found some association between the UMAP space and the total
378 range size of the species being modeled as well as its median latitude (Figure \ref{985500}). More
379 specifically I found that latitude separated species in the UMAP space, in this case with high latitude

380 species tending to be at high values of the second UMAP axis, whereas low latitude species tended
381 to have low values of UMAP 2. On the other hand, species with small ranges tended to be toward
382 the middle of the UMAP space, and larger ranged species towards the edges, forming a halo around
383 the smaller ranged species. This suggests the latent niche space has captured something ecologically
384 meaningful in its vectors. Further exploration of the meaning of these niche vectors will be conducted
in a follow-up study.

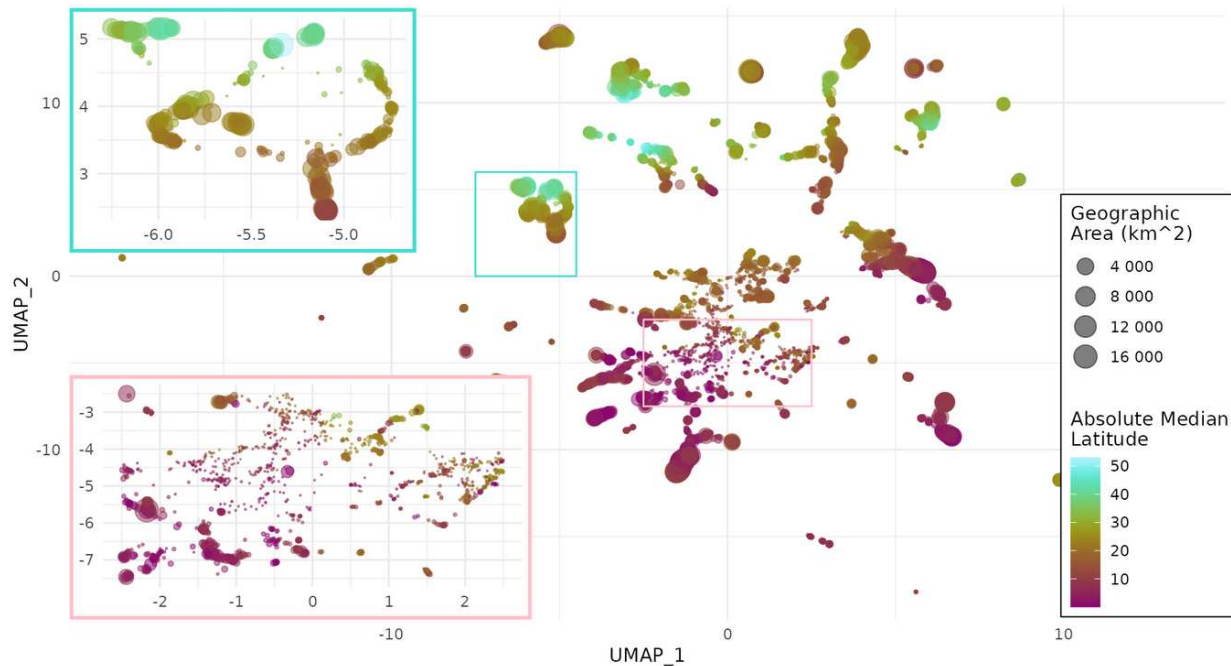


Figure 3: **UMAP visualization of the learned latent niche space for reptile species with insets showing zoomed-in regions of interest.** Each point represents a species, with its position in the latent space determined by the similarity of its inferred environmental niche. The color gradient indicates the absolute median latitude of each species' geographic range, with cooler colors representing species closer to the equator and warmer colors representing species at higher latitudes. Point size corresponds to the species' geographic range area, with larger points indicating larger ranges. The colored rectangles on the main plot correspond to zoomed-in regions displayed as insets to the left, which show greater detail of clustered species within the latent space. These clusters reveal groups of species with similar ecological niches, despite differences in their geographic regions or range sizes. This is a caption

385

386 Model evaluation metrics show NicheFlow captures geographic distributions accurately

387 The performance of the NicheFlow model was evaluated across two key scenarios: species with abundant
388 data and 'few-shot' species, where only four occurrence points were used for training. The AUC metric
389 served as the primary evaluation metric, with F-score and TSS results displaying similar trends. All
390 evaluation metrics were calculated based on a held-out sample of 400 test points per species, including

391 for the few-shot species. This consistent test sample size allowed for a robust comparison between
392 different data abundance scenarios.

393 For data-abundant species, the model exhibited strong predictive accuracy, particularly for species with
394 small and medium geographic ranges (Figure \ref{751151}). Examples of environmental and geographic
395 predictions for a randomly chosen data-abundant species can be seen in Figures 5 and 6. For evaluation
396 metrics, at high latitudes, small-range species achieved the highest mean AUC (0.99 ± 0.01). However,
397 performance for large-range species was lower across all latitudinal zones, with a notable dip at equatorial
398 latitudes (0.75 ± 0.02).

399 In the few-shot species scenario, where the model was trained on only four occurrence points, its
400 performance remained impressive. Examples of environmental and geographic predictions for a randomly
401 chosen data-abundant species can be seen in Figures 7 and 8. AUC for small-range species at high latitudes
402 achieved a value of 0.95 ± 0.01 . AUC values were also particularly high for small and medium-range
403 species in middle latitudes (0.94 ± 0.01 and 0.91 ± 0.02 , respectively). However, as seen in the data-
404 abundant species, large-range species at equatorial latitudes exhibited the lowest AUC performance
405 (0.77 ± 0.03). The consistently strong performance, even with few-shot training data, demonstrates the
406 robustness of NicheFlow in making accurate predictions for under-sampled species.

407 The lower performance observed for large-range species is likely attributable to the generative sampling
408 strategy. Large-range species require more points to adequately capture the full extent of their distributi-
409 on. With the current fixed sampling approach, some hexagonal grid cells that encompass the large-range
410 species may contain zero points due to random chance. This results in sparse geographic coverage, li-
411 miting the accuracy of predictions for large-range species. In future work, I plan to address this issue
412 by adaptively sampling more points for large-range species, iteratively sampling until cell frequencies
413 converge to a stable value. This will ensure more comprehensive coverage of large ranges, especially at
414 equatorial latitudes, where environmental heterogeneity demands more extensive sampling to accurately
415 represent species distributions. This strategy is expected to improve the model's accuracy for species
416 with expansive distributions.

417 Across all species, the model showed robust performance even for few-shot species, where only four
418 training points were available, compared with 800 points for all other species. Specifically, the average
419 AUC for data-deficient species was 0.87, while data-abundant species achieved a slightly higher average
420 AUC of 0.92. Interestingly, few-shot species exhibited a higher F-score of 0.86 compared to 0.81 for
421 data-abundant species, suggesting that the model effectively captured the general characteristics of the
422 species distributions despite extreme data deficiency. The TSS values for few-shot species, although
423 lower, still indicate a reasonable ability to differentiate presence from absence in the test data. This
424 demonstrates the model's capability of learning useful species-environment relationships, even in highly
425 data-scarce situations.

426 This held-out test set consisted of 400 points for both data-abundant and few-shot species, providing a
427 reliable evaluation of the model's predictive capacity across different data regimes. The model's gene-
428 ralization ability, particularly for species with very limited occurrence records, underscores its potential
for addressing real-world biodiversity data challenges, where species are often data-deficient.

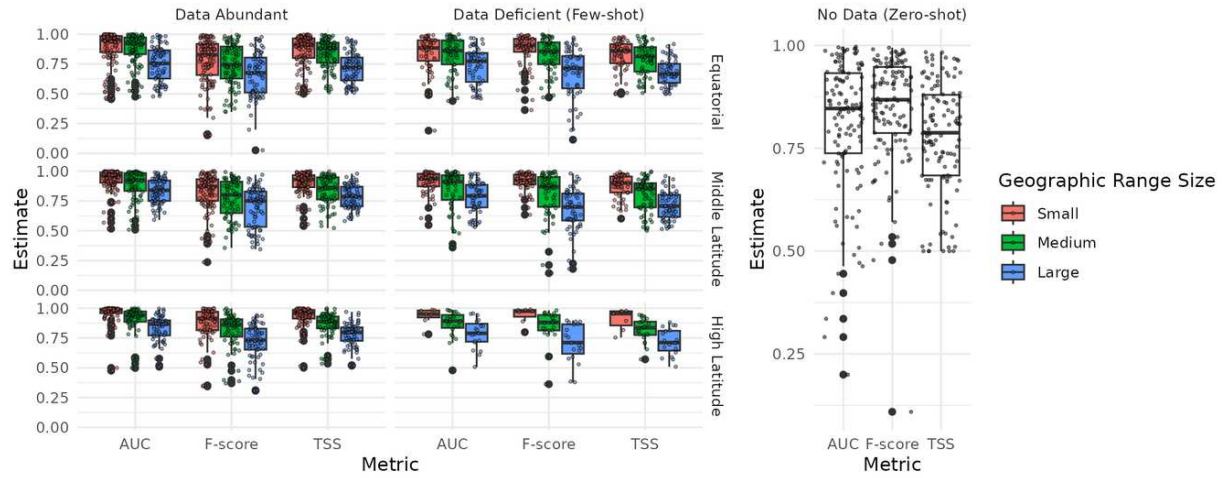


Figure 4: Evaluation of NicheFlow model performance across species with different geographic range sizes and data availability levels, measured using AUC, F-score, and TSS metrics. The left-hand panels depict results for species with abundant occurrence data, while the right-hand panels focus on 'few-shot' species, for which only 4 training points were provided. Results are further stratified by latitudinal zone (Equatorial, Middle Latitude, High Latitude) and geographic range size (Small, Medium, Large). Each boxplot summarizes the distribution of the given metric across species, with higher values indicating better performance. Note that TSS has been normalized to fall between 0 and 1 to facilitate comparison with the other metrics (normally it ranges between -1 and 1).

429

Ablepharus budaki

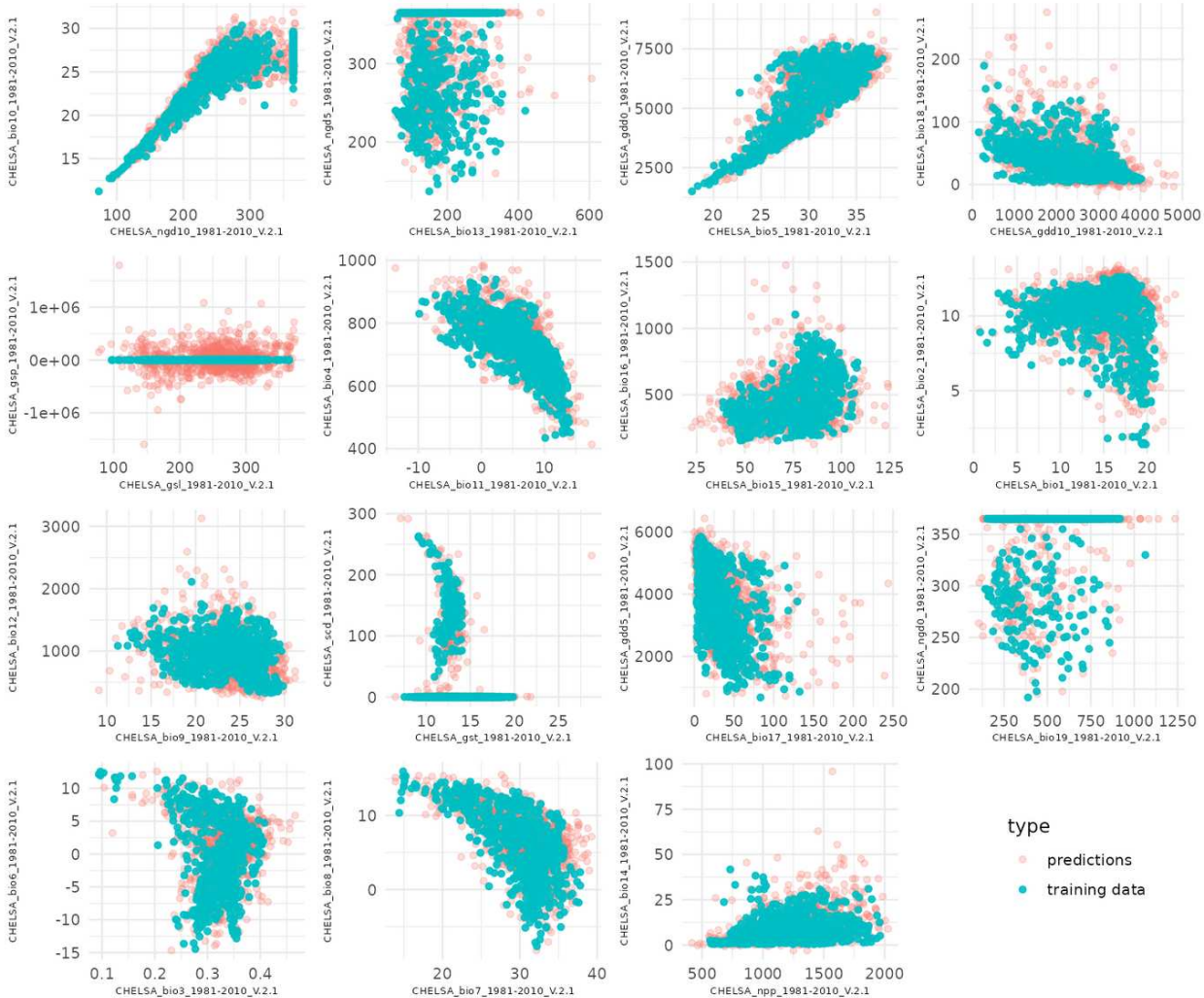
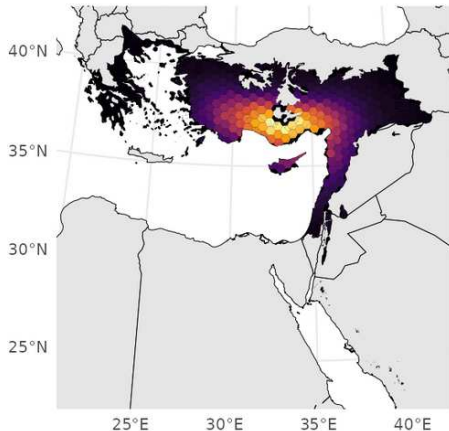


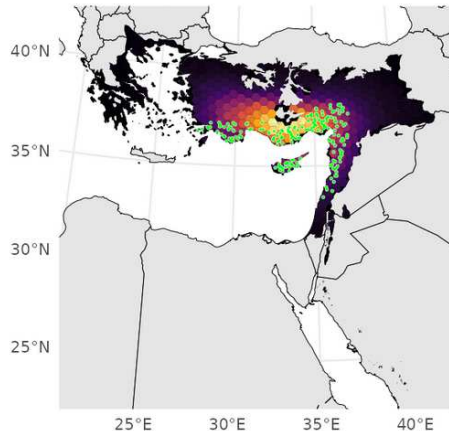
Figure 5: Environmental niche predictions for *Ablepharus budaki* showing comparisons between predicted and training data across 15 pairs of bioclimatic variables from the CHELSA dataset. Each scatterplot compares the environmental variable's predicted values (red) to the training data (blue). The model shows good alignment between predicted and observed environmental variables, demonstrating how well the model captures the environmental space associated with the species.

Ablepharus budaki

NicheFlow Predictions



Test Occurrences



Metric	Estimate
j_index	0.6477156
accuracy	0.8291457
roc_auc	0.8815921
f_meas	0.8515284
kap	0.6504262

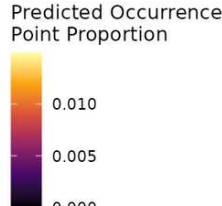


Figure 6: Geographic prediction maps for *Ablepharus budaki* comparing NicheFlow predictions to the species' true test occurrences. The left panel shows the predicted occurrence probability in hexagon bins across the species' range, while the right panel depicts the test occurrence points used for evaluation. The table below the maps summarizes the model performance metrics, with an AUC of 0.88 indicating strong predictive accuracy for this species' distribution. The inset globe highlights the species' location within its global context.

Leptosiaphos graueri

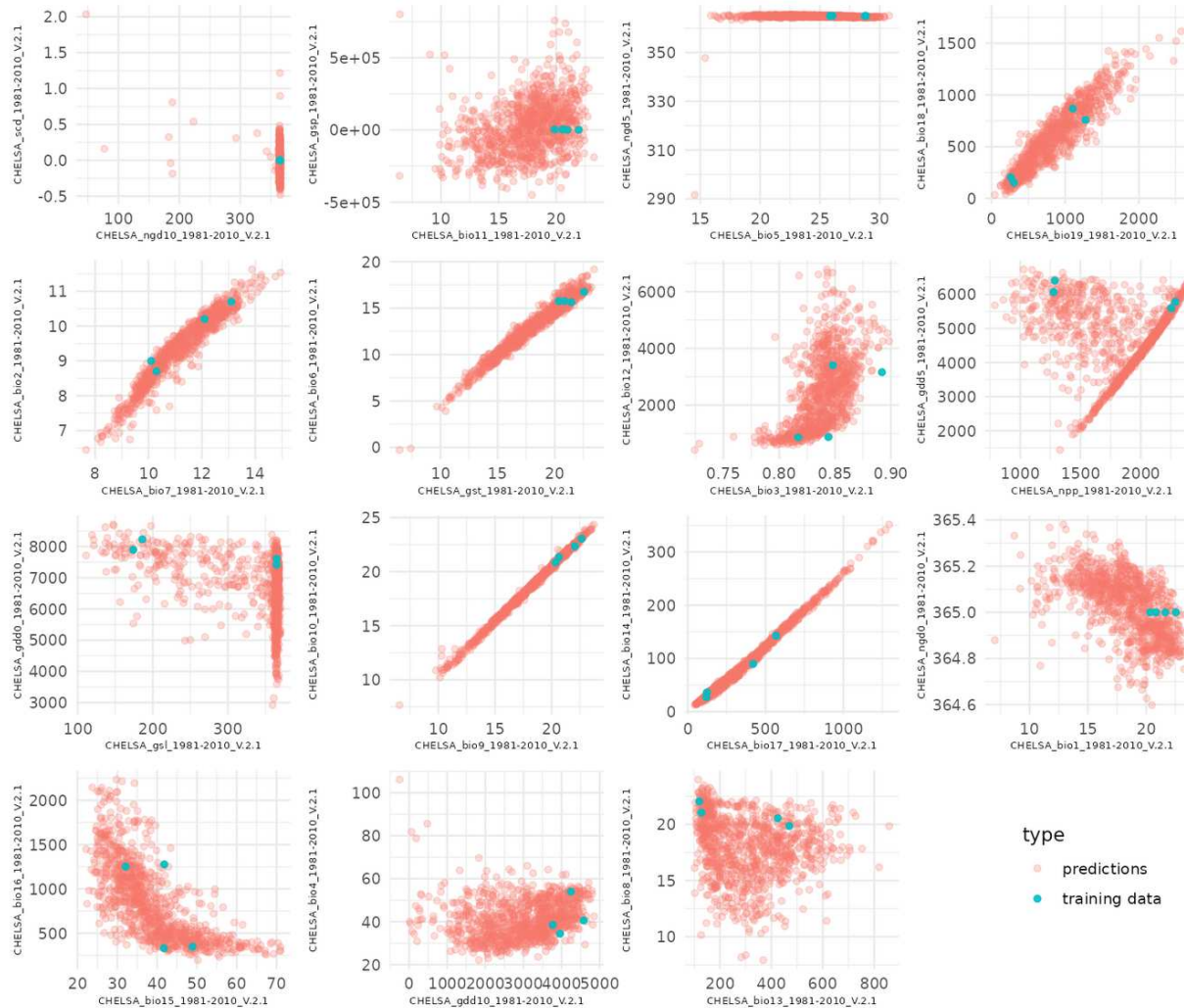


Figure 7: Plots comparing model predictions and observed occurrences in environmental space for the species *Leptosiaphos graueri*, a few-shot species with only 4 training points. Pairwise scatterplots comparing the predicted environmental variables (red) to the true occurrence data (blue). Each panel represents a different combination of 16 environmental variables sampled from the CHELSA-BIOCLIM dataset, allowing for the evaluation of the model's ability to replicate the environmental conditions associated with the species' range. This plot highlights the model's performance, particularly for species with extremely limited training data.

Leptosiaphos graueri

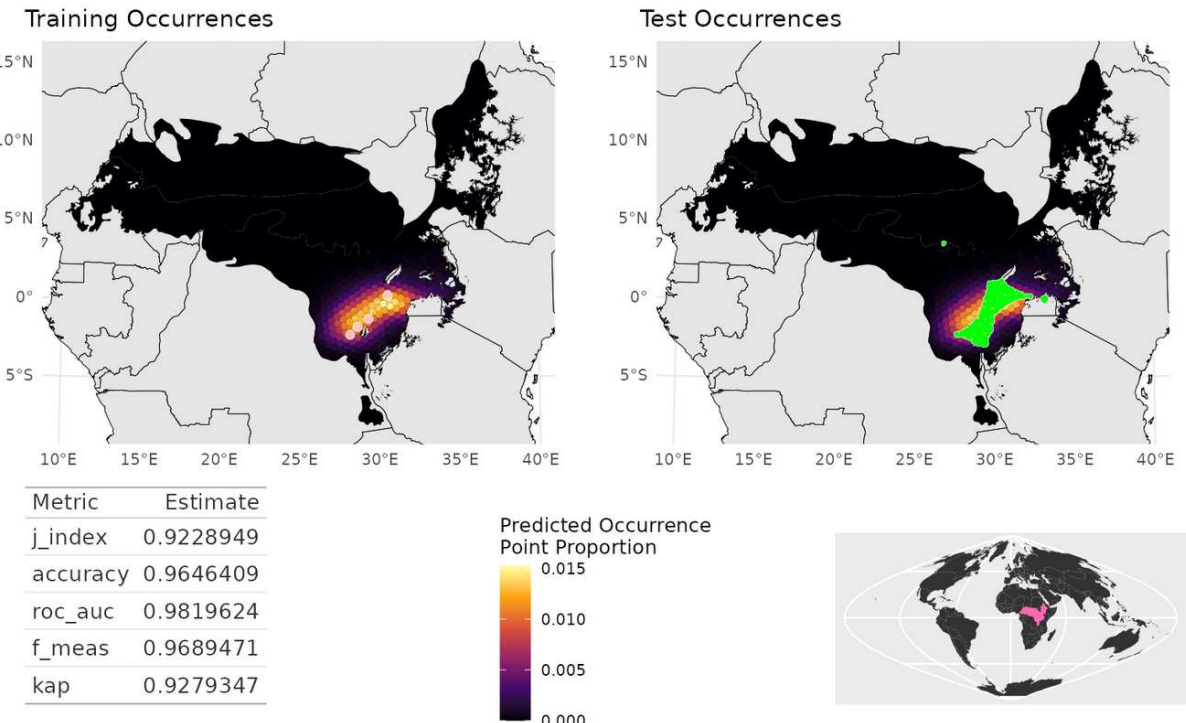


Figure 8: Maps comparing model predictions and test occurrences for the species *Leptosiaphos graueri*, a few-shot species with only 4 training points. The left panel shows the hex-binned predictions from the NicheFlow model along with the four training points in yellow, while the right panel shows the actual test occurrences (400 points). Colors indicate predicted occurrence proportions for each hexagon. The table below provides key evaluation metrics, including J-index, accuracy, ROC-AUC, F-measure, and True Skill Statistic (J-index). The inset map shows the global context for the region where this species occurs. Predictions somewhat underestimate the true extent of the range, a common occurrence for data-deficient species and probably a result of the few randomly sample location being more likely to come from the centre of the range. Nevertheless evaluation metric are very good with AUC of 0.98.

430

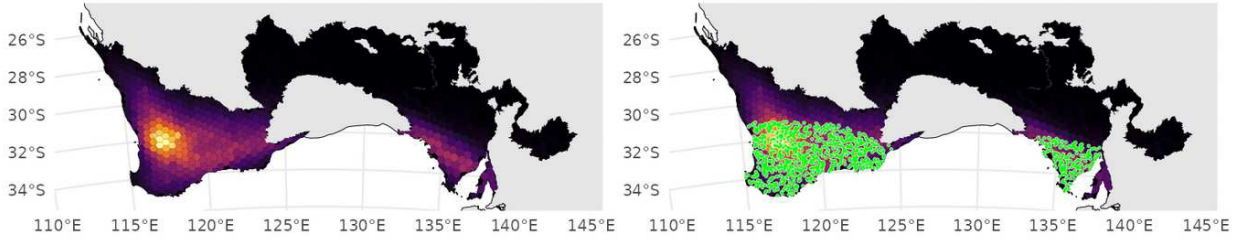
431 **NicheFlow successfully performs Zero-Shot prediction**

432 Even with species that had no data in the training set, it was possible to get good quality distribution
433 prediction from NicheFlow by match occurrence point of the species to generated occurrence point
434 distribution from the model and using this to optimize the zero-shot species latent niche space vector
435 *z_species* (Figure 9). Overall I tested 124 species that had been held-out entirely from the training set
436 (Figure 4, right panel). When tested against the 400 held-out occurrence points, on average NicheFlow
437 predicted species distribution had an AUC of 0.81 ± 0.01 (median = 0.84). This is substantially lower
438 than for data abundant or few-shot species but nevertheless remarkable considering the training sample
439 size of $N = 0$. There was also more spread for zero-shot species, with them being the only species to
440 occasionally exhibit an AUC less than 0.5, representing predictions that were worse than random. This
441 most likely occurred as a result of the latent vector optimization failing to find a good optimum, either
442 because a good optimum did not exist in the latent space, or more likely because it got stuck in a local
443 optimum in a rough loss landscape.

Bassiana trilineata

NicheFlow Predictions

Test Occurrences



Metric	Estimate
j_index	0.7360860
accuracy	0.9049531
roc_auc	0.9527085
f_meas	0.9352780
kap	0.7566246

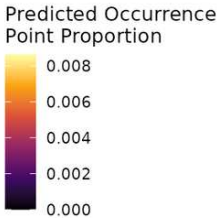


Figure 9: Zero-shot geographic predictions for Bassiana trilineata: The NicheFlow model's predicted occurrence density is shown on the left, derived entirely through zero-shot learning without training data for this species. Hexagonal bins represent the proportion of predicted occurrences, with brighter hexes indicating areas of higher predicted density. Test occurrences, shown on the right in green, are overlaid for comparison to the model's predicted points. The species' range is accurately captured despite the absence of direct training data, as reflected in high evaluation metrics, including an AUC of 0.95, F-measure of 0.93, and a True Skill Statistic (J-index) of 0.74. The bottom right inset shows the species' geographic location.

444 Discussion

445 Advancing Species Distribution Modeling with Foundation Models

446 NicheFlow represents a significant leap forward in species distribution modeling (SDM), harnessing the
447 power of generative AI to tackle long-standing challenges in ecological predictions. By employing a
448 flexible architecture capable of generalizing across species and ecosystems, NicheFlow has the potential
449 to revolutionize how we model, understand, and conserve biodiversity -- a potential foundation model
450 for ecology (Bommasani et al., 2021).

451 The application of foundation models in ecology couldn't be more timely. Traditional SDMs have long
452 grappled with limited and biased data, particularly the absence of true absence data (Elith et al., 2006).

453 NicheFlow addresses this challenge head-on by integrating species embeddings, allowing for "strength
454 sharing" between species. This innovative approach enhances predictions for rare or data-limited species,
455 building upon joint species distribution models (JSDMs) that leverage species correlations (Warton et
456 al., 2015; Pollock et al., 2014; Ovaskainen et al., 2016). However, NicheFlow goes a step further,
457 enabling non-linear generalization and thus capturing more complex ecological relationships.

458 One of NicheFlow's key strengths lies in its ability to extract patterns from large, heterogeneous datasets.
459 This capability could provide a transferable understanding of niche space, enabling predictions in new
460 regions or under future climate scenarios. Once trained and released the power of the model can be
461 utilized or fine-tuned by anyone in the research or practitioner community. Such transferability and
462 share-ability aligns perfectly with growing calls for open science and data sharing in ecology (McKiernan
463 et al., 2016; Hampton et al., 2015), extending it beyond data to model too, and paving the way for
464 more collaborative and comprehensive computational ecology research.

465 **Generative Approach: A Paradigm Shift in SDM**

466 NicheFlow marks a paradigm shift in species distribution modeling. Unlike traditional SDMs that
467 operate within a discriminative framework (Guisan & Thuiller, 2005; Franklin, 2010; Araújo & Peterson,
468 2012), NicheFlow explicitly models the conditional distribution of species in environmental space, an
469 approach with some similarities to environmental density estimation methods like hypervolume (Blonder
470 et al. 2018), but using a generative multi-species approach (see Supporting Information for a detailed
471 discussion of connections between NicheFlow and other SDM approaches). The generative approach of
472 NicheFlow offers significant advantages, particularly in handling novel climates and predicting species
473 responses to changing conditions (Araújo & Rahbek, 2006; Warren et al., 2014).

474 Perhaps the most remarkable outcome of this approach is NicheFlow's effectiveness in predicting distri-
475 butions for data-deficient or few-shot species. Few-shot learning, the ability to generalize with limited
476 examples (Wang et al., 2020), is crucial in ecology where many species have sparse occurrence records
477 (Breiner et al., 2015). NicheFlow's latent niche space allows it to leverage patterns learned from data-
478 rich species to benefit data-deficient ones. The result? Robust predictions (average AUC > 0.85) for
479 few-shot species, a feat that traditional SDMs often struggle to achieve.

480 Taking this a step further, NicheFlow demonstrates potential for zero-shot learning, predicting distri-
481 butions for species entirely absent from the training data. This capability extends the model's utility
482 dramatically, allowing researchers and practitioners to use it without retraining, regardless of data availa-
483 bility.

484 **Addressing Climate Change and Conservation Challenges**

485 In the face of rapid climate change, NicheFlow's flexibility in simulating species responses under novel
486 conditions offers a significant advantage. Traditional SDMs often struggle with non-analog climates
487 (Williams & Jackson, 2007), but NicheFlow's generative approach may better capture species' potential
488 responses to new environmental combinations. This capability could prove invaluable in identifying future
489 suitable habitats for species reintroductions or in conservation planning (Guisan et al., 2013; Hannah et
490 al., 2007).

491 Moreover, NicheFlow's joint species distribution capabilities provide a powerful tool for community-level
492 conservation planning. By modeling multiple species simultaneously, we can identify high-biodiversity
493 regions or at-risk species assemblages more effectively (Pereira et al., 2010). This aligns perfectly with
494 global biodiversity initiatives aiming to preserve ecosystem integrity (Convention on Biological Diversity,
495 2021), offering a more holistic approach to conservation.

496 **New Frontiers in Niche Theory and Community Ecology**

497 NicheFlow's architecture opens up exciting new avenues for exploring fundamental questions in niche
498 theory. Its ability to capture complex, non-linear relationships in high-dimensional environmental space
499 aligns beautifully with Hutchinson's n-dimensional hypervolume concept (Hutchinson, 1957; Blonder,
500 2018; Holt, 2009). By examining the learned embedding space, we could gain unprecedented insights
501 into niche dimensionality, breadth, overlap, and evolution across taxa.

502 The model's capacity to generate samples from species' environmental niches enables novel approaches
503 to studying niche dynamics. This could reveal patterns of niche conservatism or divergence (Wiens et
504 al., 2010; Pearman et al., 2008), shedding light on long-standing questions in evolutionary ecology. Fur-
505 thermore, it could facilitate exploration of community assembly processes, allowing us to test hypotheses
506 about environmental filtering versus competitive exclusion (Kraft et al., 2015; Cadotte & Tucker, 2017)
507 with greater precision than ever before.

508 NicheFlow's ability to generate hypothetical species distributions based on interpolations in the em-
509 bedding space opens up fascinating possibilities for evolutionary research. We could simulate potential
510 distributions of hybrid species or explore "empty niche space" (Schluter, 2000), providing new insights
511 into adaptive radiation and niche evolution. By combining NicheFlow with ancestral niche reconstruc-
512 tion techniques, we could even predict historical species distributions, offering new avenues for testing
513 biogeographic and niche evolution hypotheses (Wiens & Graham, 2005; Crisp & Cook, 2012; Kozak &
514 Wiens, 2006).

515 **Caveats and Future Directions**

516 Despite its advancements, NicheFlow is not without limitations. The quality and biases of input data,
517 whether from expert range maps or occurrence records, can significantly impact model outcomes (Hurl-
518 bert & Jetz, 2007; Newbold, 2010; Hijmans et al., 2000; Reddy & Dávalos, 2003). To address this,
519 future iterations of NicheFlow should leverage multiple data types, creating more comprehensive and
520 nuanced representations of species distributions.

521 Interpretability remains a challenge, as with many deep learning models in ecology (Merow et al., 2014;
522 Olden et al., 2008). To enhance NicheFlow's utility for ecological insight, we must focus on improving
523 model interpretability. This could involve incorporating explainable AI techniques or developing methods
524 to translate learned embeddings into ecologically meaningful concepts.

525 To provide a more nuanced view of species' ecological niches, it will be critical to better incorporate
526 uncertainty into NicheFlow. We can achieve this by implementing a variational autoencoder variant to
527 model the latent space, facilitating better uncertainty quantification in model predictions. This probabi-
528 listic treatment will also enable more effective amortized inference, potentially improving computational
529 efficiency.

530 Enhancing zero-shot prediction capabilities represents another key area for improvement. By increa-
531 sing latent space regularization and incorporating auxiliary predictors such as phylogenetic information,
532 species traits, and environmental data, we can significantly expand NicheFlow's utility in predicting
533 distributions for rare, newly discovered, or data-deficient species.

534 To truly realize the potential of a foundation model in ecology, we aim to train NicheFlow on distribution
535 data for all terrestrial vertebrates in the next phase of development. This comprehensive dataset will
536 allow the model to capture a wider range of ecological niches and biogeographic patterns, enabling more
537 robust exploration of macroecological patterns and cross-taxa comparisons.

538 **Ethical Considerations**

539 As we advance this powerful tool, we must not overlook important ethical and societal considerations.
540 Issues of data privacy and ownership, particularly for data from indigenous communities or citizen
541 scientists, necessitate clear guidelines on data usage and sharing (Groom et al., 2017). We must also
542 carefully consider how to share and use model outputs to prevent potential misuse, such as exploitation
543 by poachers or land grabbers.

544 Ensuring equitable access to NicheFlow is crucial. We must address potential exacerbation of existing
545 inequalities in ecological research and conservation planning due to computational resource requirements.
546 By democratizing access to this advanced tool, we can foster more inclusive and comprehensive global
547 biodiversity research and conservation efforts.

548 Conclusion

549 NicheFlow represents a significant step forward in species distribution modeling, offering new insights
550 into ecological niches and species distributions. As we continue to refine and expand the model, its
551 potential applications in climate change impact assessment, conservation planning, and evolutionary
552 studies are vast. The integration of NicheFlow with other data sources promises to further enhance our
553 understanding of biodiversity patterns and processes, providing crucial tools for addressing mounting
554 ecological challenges in the face of global change. By leveraging the power of foundation models and
555 generative AI, NicheFlow paves the way for a new era in ecological modeling and conservation planning.

556 References

557 Araújo, M. B., & Peterson, A. T. (2012). Uses and misuses of bioclimatic envelope modeling. *Ecology*,
558 93(7), 1527-1539.

559 Araújo, M. B., & Rahbek, C. (2006). How does climate change affect biodiversity? *Science*, 313(5792),
560 1396-1397.

561 Beery, S., Cole, E., Parker, J., Perona, P., & Winner, K. (2021). Species distribution modeling for machi-
562 ne learning practitioners: A review. In *Proceedings of the 4th ACM SIGCAS Conference on Computing*
563 *and Sustainable Societies* (pp. 329-348).

564 Bini, L. M., Diniz-Filho, J. A. F., Rangel, T. F., Bastos, R. P., & Pinto, M. P. (2006). Challenging
565 Wallacean and Linnean shortfalls: Knowledge gradients and conservation planning in a biodiversity
566 hotspot. *Global Ecology and Biogeography*, 15(1), 47-52.

567 Blonder, B. (2018). Hypervolume concepts in niche-and trait-based ecology. *Ecography*, 41(9), 1441-
568 1455.

569 Blonder, B., Morrow, C. B., Maitner, B., Harris, D. J., Lamanna, C., Violle, C., Enquist, B. J., &
570 Kerkhoff, A. J. (2018). New approaches for delineating n-dimensional hypervolumes. *Methods in*
571 *Ecology and Evolution*, 9(2), 305-319

572 Bommasani, R., Hudson, D. A., Adeli, E., Altman, R., Arora, S., von Arx, S., ... & Liang, P. (2021).
573 On the opportunities and risks of foundation models. *arXiv preprint*, arXiv:2108.07258.

574 Breiner, F. T., Guisan, A., Bergamini, A., & Nobis, M. P. (2015). Overcoming limitations of modelling
575 rare species by using ensembles of small models. *Methods in Ecology and Evolution*, 6(10), 1210-1218.

576 Brodrick, P. (2019). *h3: Bindings to Uber's H3 Geospatial Indexing System*. Available at <https://CRAN.R-project.org/package=h3>.

578 Cadotte, M. W., & Tucker, C. M. (2017). Should environmental filtering be abandoned? *Trends in*
579 *Ecology & Evolution*, 32(6), 429-437.

580 Convention on Biological Diversity. (2021). *First Draft of the Post-2020 Global Biodiversity Framework*.
581 CBD/WG2020/3/3.

582 Crisp, M. D., & Cook, L. G. (2012). Phylogenetic niche conservatism: What are the underlying
583 evolutionary and ecological causes? *New Phytologist*, 196(3), 681-694.

584 Dai, B., & Wipf, D. (2019). Diagnosing and enhancing VAE models. *arXiv preprint*, arXiv:1903.05789.

585 Elith, J., Graham, C. H., Anderson, R. P., Dudik, M., Ferrier, S., Guisan, A., ... & Zimmermann, N. E.
586 (2006). Novel methods improve prediction of species' distributions from occurrence data. *Ecography*,
587 29(2), 129-151.

588 Elith, J., & Leathwick, J. R. (2009). Species distribution models: Ecological explanation and prediction
589 across space and time. *Annual Review of Ecology, Evolution, and Systematics*, 40, 677-697.

590 Feeley, K. J., & Silman, M. R. (2011). The data void in modeling current and future distributions of
591 tropical species. *Global Change Biology*, 17(1), 626-630.

592 Fithian, W., Elith, J., Hastie, T., & Keith, D. A. (2015). Bias correction in species distribution models:
593 pooling survey and collection data for multiple species. *Methods in Ecology and Evolution*, 6(4), 424-
594 438.

595 Fitzpatrick, M. C., & Hargrove, W. W. (2009). The projection of species distribution models and the
596 problem of non-analog climate. *Biodiversity and Conservation*, 18(8), 2255-2261.

597 Franklin, J. (2010). *Mapping species distributions: Spatial inference and prediction*. Cambridge Uni-
598 versity Press.

599 Grattarola, F., Bowler, D. E., & Keil, P. (2023). Integrating presence-only and presence-absence data
600 to model changes in species geographic ranges: An example in the Neotropics. *Journal of Biogeography*,
601 50(9), 1561-1575.

602 Groom, Q., Weatherdon, L., & Geijzendorffer, I. R. (2017). Is citizen science an open science in the
603 case of biodiversity observations?. *Journal of Applied Ecology*, 54(2), 612-617.

604 Guisan, A., Thuiller, W., & Zimmermann, N. E. (2017). *Habitat suitability and distribution models:
605 with applications in R*. Cambridge University Press.

606 Guisan, A., & Thuiller, W. (2005). Predicting species distribution: Offering more than simple habitat
607 models. *Ecology Letters*, 8(9), 993-1009.

608 Guisan, A., Tingley, R., Baumgartner, J. B., Naujokaitis-Lewis, I., Sutcliffe, P. R., Tulloch, A. I., ...
609 & Buckley, Y. M. (2013). Predicting species distributions for conservation decisions. *Ecology Letters*,

610 16(12), 1424-1435.

611 Hampton, S. E., Strasser, C. A., Tewksbury, J. J., Gram, W. K., Budden, A. E., Batcheller, A. L., ...
612 & Porter, J. H. (2015). The Tao of open science for ecology. *Ecosphere*, 6(7), 1-13.

613 Hannah, L., Midgley, G., Andelman, S., Araujo, M., Hughes, G., Martinez-Meyer, E., ... & Williams,
614 P. (2007). Protected area needs in a changing climate. *Frontiers in Ecology and the Environment*, 5(3),
615 131-138.

616 Hijmans, R. J., Garrett, K. A., Huaman, Z., Zhang, D. P., Schreuder, M., & Bonierbale, M. (2000).
617 Assessing the geographic representation of gene bank collections: The case of Bolivian wild potatoes.
618 *Conservation Biology*, 14(6), 1755-1765.

619 Hoffmann, A. A., & Sgro, C. M. (2011). Climate change and evolutionary adaptation. *Nature*,
620 470(7335), 479-485.

621 Holt, R. D. (2009). Bringing the Hutchinsonian niche into the 21st century: Ecological and evolutionary
622 perspectives. *Proceedings of the National Academy of Sciences*, 106(Supplement 2), 19659-19665.

623 Hutchinson, G. E. (1957). Concluding remarks. *Cold Spring Harbor Symposia on Quantitative Biology*,
624 22, 415-427.

625 Jetz, W., Thomas, G. H., Joy, J. B., Hartmann, K., & Mooers, A. O. (2012). The global diversity of
626 birds in space and time. *Nature*, 491(7424), 444-448.

627 Karger, D., Conrad, O., Bohner, J. *et al.* Climatologies at high resolution for the earth's land surface
628 areas. *Sci Data* 4, 170122 (2017)

629 Kozak, K. H., & Wiens, J. J. (2006). Does niche conservatism promote speciation? A case study in
630 North American salamanders. *Evolution*, 60(12), 2604-2621.

631 Kraft, N. J., Adler, P. B., Godoy, O., James, E. C., Fuller, S., & Levine, J. M. (2015). Community
632 assembly, coexistence and the environmental filtering metaphor. *Functional Ecology*, 29(5), 592-599.

633 Kuhn, M., & Wickham, H. (2020). *Tidymodels: A collection of packages for modeling and machine*
634 *learning using tidyverse principles*. Available at <https://www.tidymodels.org>.

635 LeCun, Y., Bengio, Y., & Hinton, G. (2015). Deep learning. *Nature*, 521(7553), 436-444.

636 Liu, W., Tian, Y., & Ren, W. (2023). Flow straight and fast: Learning to generate and transfer data
637 with rectified flow. *arXiv preprint*, arXiv:2209.03003.

638 McKiernan, E. C., Bourne, P. E., Brown, C. T., Buck, S., Kenall, A., Lin, J., ... & Yarkoni, T. (2016).
639 How open science helps researchers succeed. *eLife*, 5, e16800.

640 Merow, C., Smith, M. J., & Silander, J. A. (2014). A practical guide to MaxEnt for modeling species'
641 distributions: what it does, and why inputs and settings matter. *Ecography*, 37(10), 1058-1069.

642 Newbold, T. (2010). Applications and limitations of museum data for conservation and ecology, with
643 particular attention to species distribution models. *Progress in Physical Geography*, 34(1), 3-22.

644 Norberg, A., Abrego, N., Blanchet, F. G., Adler, F. R., Anderson, B. J., Anttila, J., ... & Ovaskainen,
645 O. (2019). A comprehensive evaluation of predictive performance of 33 species distribution models at
646 species and community levels. *Ecological Monographs*, 89(3), e01370.

647 Nogués-Bravo, D. (2009). Predicting the past distribution of species climatic niches. *Global Ecology*
648 and Biogeography

649 Olden, J. D., Lawler, J. J., & Poff, N. L. (2008). Machine learning methods without tears: A primer
650 for ecologists. *The Quarterly Review of Biology*, 83(2), 171-193

651 Ovaskainen, O., Abrego, N., Halme, P., & Dunson, D. (2016). Using latent variable models to identify
652 large networks of species-to-species associations at different spatial scales. *Ecology*, 97(1), 61-70.

653 Ovaskainen, O., Tikhonov, G., Norberg, A., Guillaume Blanchet, F., Duan, L., Dunson, D., ... &
654 Abrego, N. (2017). How to make more out of community data? A conceptual framework and its
655 implementation as models and software. *Ecology Letters*, 20(5), 561-576.

656 Pebesma, E. (2018). Simple features for R: Standardized support for spatial vector data. *The R Journal*,
657 10(1), 439-446. <https://doi.org/10.32614/RJ-2018-009>

658 Pearman, P. B., Guisan, A., Broennimann, O., & Randin, C. F. (2008). Niche dynamics in space and
659 time. *Trends in Ecology & Evolution*, 23(3), 149-158.

660 Pecl, G. T., Araujo, M. B., Bell, J. D., Blanchard, J., Bonebrake, T. C., Chen, I. C., ... & Williams,
661 S. E. (2017). Biodiversity redistribution under climate change: Impacts on ecosystems and human
662 well-being. *Science*, 355(6332), eaai9214.

663 Pereira, H. M., Leadley, P. W., Proenca, V., Alkemade, R., Scharlemann, J. P., Fernandez-Manjarres, J.
664 F., ... & Walpole, M. (2010). Scenarios for global biodiversity in the 21st century. *Science*, 330(6010),
665 1496-1501.

666 Phillips, S. J., Anderson, R. P., & Schapire, R. E. (2006). Maximum entropy modeling of species
667 geographic distributions. *Ecological Modelling*, 190(3-4), 231-259.

668 Pimm, S. L., Jenkins, C. N., Abell, R., Brooks, T. M., Gittleman, J. L., Joppa, L. N., ... & Sexton,
669 J. O. (2015). The biodiversity of species and their rates of extinction, distribution, and protection.
670 *Science*, 344(6187), 1246752.

671 Pollock, L. J., Tingley, R., Morris, W. K., Golding, N., O'Hara, R. B., Parris, K. M., ... & McCarthy,

672 M. A. (2014). Understanding co-occurrence by modelling species simultaneously with a joint species
673 distribution model (JSDM). *Methods in Ecology and Evolution*, 5(5), 397-406.

674 Reichstein, M., Camps-Valls, G., Stevens, B., Jung, M., Denzler, J., Carvalhais, N., & Prabhat. (2019).
675 Deep learning and process understanding for data-driven Earth system science. *Nature*, 566(7743),
676 195-204.

677 Reddy, S., & Dávalos, L. M. (2003). Geographical sampling bias and its implications for conservation
678 priorities in Africa. *Journal of Biogeography*, 30(11), 1719-1727.

679 Roll, U., Feldman, A., Novosolov, M., et al. (2017). The global distribution of tetrapods reveals a need
680 for targeted reptile conservation. *Nature Ecology & Evolution*, 1, 1677–1682. <https://doi.org/10.1038/s41559-017-0332-2>

682 Sanh, V., Debut, L., Chaumond, J., & Wolf, T. (2019). DistilBERT, a distilled version of BERT:
683 Smaller, faster, cheaper and lighter. *arXiv preprint*, arXiv:1910.01108.

684 Schlüter, D. (2000). *The ecology of adaptive radiation*. Oxford University Press.

685 Soberón, J. (2007). Grinnellian and Eltonian niches and geographic distributions of species. *Ecology*
686 *Letters*, 10(12), 1115-1123.

687 Soberón, J., & Peterson, A. T. (2005). Interpretation of models of fundamental ecological niches and
688 species' distributional areas. *Biodiversity Informatics*, 2, 1-10.

689 Steen, V. A., Elphick, C. S., & Tingley, M. W. (2019). An evaluation of stringent filtering to improve
690 species distribution models from citizen science data. *Diversity and Distributions*, 25(12), 1857-1869.

691 Strubell, E., Ganesh, A., & McCallum, A. (2019). Energy and policy considerations for deep learning
692 in NLP. *Proceedings of the 57th Annual Meeting of the Association for Computational Linguistics*,
693 3645-3650.

694 Urban, M. C., Bocedi, G., Hendry, A. P., Mihoub, J. B., Pe'er, G., Singer, A., ... & Travis, J. M.
695 (2016). Improving the forecast for biodiversity under climate change. *Science*, 353(6304), aad8466.

696 Vaughan, D. (2020). *probably: Tools for post-processing class probability estimates*. Available at
697 <https://CRAN.R-project.org/package=probably>.

698 Wang, Y., Gonzalez-Garcia, A., Berga, D., et al. (2020). MineGAN: Effective knowledge transfer from
699 GANs to target domains with few images. *Proceedings of the 2020 IEEE Conference on Computer*
700 *Vision and Pattern Recognition*, 9329-9338.

701 Warton, D. I., Blanchet, F. G., O'Hara, R. B., Ovaskainen, O., Taskinen, S., Walker, S. C., & Hui, F. K.
702 C. (2015). So many variables: Joint modeling in community ecology. *Trends in Ecology & Evolution*,
703 30(12), 766-779.

704 Wiens, J. J., & Graham, C. H. (2005). Niche conservatism: Integrating evolution, ecology, and conser-
705 vation biology. *Annual Review of Ecology, Evolution, and Systematics*, 36, 519-539.

706 Wiens, J. J., Ackerly, D. D., Allen, A. P., Anacker, B. L., Buckley, L. B., Cornell, H. V., ... & Stephens,
707 P. R. (2010). Niche conservatism as an emerging principle in ecology and conservation biology. *Ecology*
708 *Letters*, 13(10), 1310-1324.

709 Williams, J. W., & Jackson, S. T. (2007). Novel climates, no-analog communities, and ecological
710 surprises. *Frontiers in Ecology and the Environment*, 5(9), 475-482.

711 Wisz, M. S., Pottier, J., Kissling, W. D., Pellissier, L., Lenoir, J., Damgaard, C. F., ... & Svenning, J.
712 C. (2013). The role of biotic interactions in shaping distributions and realised assemblages of species:
713 Implications for species distribution modelling. *Biological Reviews*, 88(1), 15-30.

714 Xian, Y., Lampert, C. H., Schiele, B., & Akata, Z. (2018). Zero-shot learning—a comprehensive
715 evaluation of the good, the bad and the ugly. *IEEE Transactions on Pattern Analysis and Machine*
716 *Intelligence*, 41(9), 2251-2265.

717 Yackulic, C. B., Chandler, R., Zipkin, E. F., Royle, J. A., Nichols, J. D., Campbell Grant, E. H., & Veran,
718 S. (2013). Presence-only modelling using MAXENT: When can we trust the inferences? *Methods in*
719 *Ecology and Evolution*, 4(3), 236-243.

720 Youden, W. J. (1950). Index for rating diagnostic tests. *Cancer*, 3(1), 32-35.

721 Zheng, Y., He, T., Qiu, Y., & Wipf, D.P. (2023). Learning Manifold Dimensions with Conditional
722 Variational Autoencoders. *ArXiv*, abs/2302.11756.

723 Data Availability

724 All code used to implement the NicheFlow model is publicly available on Github. Data use to train a
725 proof-of-principle model is available publicly at [https://datadryad.org/stash/dataset/doi:10.](https://datadryad.org/stash/dataset/doi:10.5061/dryad.83s7k)
726 [5061/dryad.83s7k](https://datadryad.org/stash/dataset/doi:10.5061/dryad.83s7k) and <https://chelsa-climate.org/bioclim/>

727 Code for implementing the models is publicly available on GitHub (<https://github.com/rdinnager/genAISDM>)

729 Supporting Information

730 A supporting information document can be found at [https://www.authorea.com/users/5518/](https://www.authorea.com/users/5518/articles/1231655-nicheflow-towards-a-foundation-model-for-species-distribution-modelling-supporting-information)
731 [articles/1231655-nicheflow-towards-a-foundation-model-for-species-distribution-](https://www.authorea.com/users/5518/articles/1231655-nicheflow-towards-a-foundation-model-for-species-distribution-modelling-supporting-information)
732 [modelling-supporting-information](https://www.authorea.com/users/5518/articles/1231655-nicheflow-towards-a-foundation-model-for-species-distribution-modelling-supporting-information)

⁷³³ This includes an animated figure demonstrating latent niche interpolation for the NicheFlow reptile
⁷³⁴ model.